

Structural analysis of graphene oxide/silver nanocomposites: optical properties, electrochemical sensing and photocatalytic activity

Manish Kumar^{1,2} · Unni Krishnan² · Pooja Devi¹ · Akshay Kumar² 

Received: 4 August 2017 / Accepted: 18 September 2017 / Published online: 26 September 2017
© Springer Science+Business Media, LLC 2017

Abstract In the present study, graphene oxide/silver (GO/Ag) nanocomposites were synthesized via a facile simple one pot chemical reduction method using ethylene glycol/sodium borohydrate (EG/NaBH₄) as solvent and reducing agent. GO was selected as a substrate and stabilizer to prepare GO/Ag nanocomposites. The synthesized GO/Ag nanocomposites were characterized by a series of techniques. Highly monodispersed stable crystalline silver nanoparticles having a face-centered cubic (fcc) phase were confirmed by X-ray powder diffraction (XRD) on GO signature. Scanning electron microscopy images showed that Ag nanoparticles are deposited on the GO sheet with a narrow size distribution. Transmission electron microscopy observations revealed that large numbers of Ag nanoparticles were uniformly distributed on GO sheet and well separated with an average size of 18 nm. Ultraviolet–visible (UV–Vis) spectroscopic results showed the peak of GO and surface plasmon resonance (SPR) of Ag nanoparticles. The SPR property of GO/Ag nanocomposites showed that there was an interaction between Ag nanoparticles and GO sheet. The intensities of the Raman signal of GO/Ag nanocomposites are gradually increased with attachment of Ag nanoparticles i.e. there is surface-enhanced Raman scattering activity. Electrochemical investigations indicated that the nanocomposites possessed an excellent performance for detecting towards 4-nitrophenol. An application of the obtained GO/Ag nanocomposites as a catalyst in the reduction of 4-nitrophenol to

4-aminophenol by NaBH₄ was demonstrated. The GO/Ag nanocomposites exhibited high activity and stability for the catalytic reduction of 4-nitrophenol. The prepared GO/Ag nanocomposites act as photo-catalysts.

1 Introduction

Graphene is a 2-dimensional extended honeycomb network of sp²-hybridized carbon [1] which makes it thinnest known material in the universe. Graphene has attracted considerable scientific attention on account of its unique properties, such as high specific surface area (2630 m²/g), excellent mechanical strength, thermal and chemical properties, high electron mobility (200,000 cm² V⁻¹ s⁻¹), high electrical conductivity (10³–10⁴ S/m) [2–4]. GO has strong hydrophilic ability due to the large number of oxygen bonds in its edges and defective sites, such as carboxylic (–COOH), hydroxyl (C–OH), carbonyl (C=O), and epoxide groups (C–O–C) [5]. Its hydrophilic ability contributes to forming stable colloidal dispersions in water [6]. Moreover, those functional groups have been confirmed to own reducibility [7] and have been actively used to build new graphene decorated composites with inorganic nanoparticles, such as MgO, ZnO, Ag, Fe₃O₄, Pt etc [8–12]. In particular, GO/Ag nanocomposites have attracted tremendous interest because of its optical [13], electrochemical properties [14] and high catalytic activity [15]. So far, many synthesis routes, such as, chemical reduction [16], thermal reduction [17], electrodeposition [18], and two-phase process [19], have been used to prepare GO/Ag nanocomposite. Among them, the chemical reduction method is the most promising synthesis route owing to its simple, cost-effective, efficiency, high yield.

An aromatic phenolic compound, 4-nitrophenolis is one of the toxic and pollutant substances commonly used

✉ Akshay Kumar
akshaykumar.tiet@gmail.com

¹ CSIR-Central Scientific Instruments Organisation,
Chandigarh 160030, India

² Sri Guru Granth Sahib World University,
Fatehgarh Sahib 140406, India

as pesticide and insecticide [20]. Therefore, the monitoring and selective determination of 4-nitrophenol becomes more significant to both environmental and human safety aspects. Many analytical methods have been prepared for determining 4-nitrophenol, such as spectrophotometry [21], fluorescence [22], high performance liquid chromatography [23], and electrochemical technique [24]. Among these techniques, electrochemical method was found to have advantages of fast response, cost effective instrument, simple operation, time saving, high sensitivity and selectivity, real-time detection for real samples [25, 26]. However, the electrochemical reduction of 4-nitrophenol at a bare electrode is generally difficult and needs a high over potential. Herein, we report a facile chemical reduction method for synthesis of GO/Ag nanocomposites by direct reduction of AgNO_3 on GO sheet with EG and NaBH_4 . It is worth highly lighting that the reaction process did not require a vacuum or inert atmosphere, temperature and can be further analysed with in situ characterization for their morphology, optical, electrochemical and catalytic properties. The GO/Ag nanocomposites modified electrode was then used for electrochemical sensing towards 4-nitrophenol. In addition, photo-catalytic activity was also investigated for these nanocomposites. The incorporation of Ag nanoparticles with GO significantly improved the catalytic activity for the reduction of 4-nitrophenol by NaBH_4 in comparison with the Ag nanoparticles.

2 Experimental

2.1 Materials

All chemicals purchased were of analytical reagent grade and used without further purification. Graphite powder was procured from Sigma-Aldrich. Silver nitrate (AgNO_3 , 99.8%), potassium permanganate (KMnO_4 , 99.9%), hydrogen peroxide (H_2O_2 , 30%), hydrochloric acid (HCl , 37% w/v), sodium borohydrate (NaBH_4 , 99.99%) and sulphuric acid (H_2SO_4 , 98%) were obtained from Merck Specialties Pvt. Ltd. *O*-phosphoric acid (H_3PO_4 , 85%) and ethylene glycol (EG; $\text{C}_2\text{H}_6\text{O}_2$, 98%) were purchased from Fisher Scientific Pvt. Ltd., 4-nitrophenol was acquired from Loba Chemie Pvt. Ltd. Deionised (DI) water obtained from Millipore (resistivity 18 $\text{M}\Omega$ cm) was used throughout this study.

2.2 Instrumentation

The crystal phase and microstructure of the synthesized product was determined by powder X-ray diffraction (XRD) technique with Pananalytical X'Pert Pro powder X-ray diffractometer. The X-ray pattern was recorded at room temperature using monochromatic CuK_α radiation ($\lambda = 105,418 \text{ \AA}$)

to generate diffraction patterns from powder crystalline sample at ambient temperature in a 2θ range of 10° – 80° at a scan speed of 5° min^{-1} . FTIR spectra of sample were collected on Varian FTIR system (600 series, USA) in the frequency range 500 – 4000 cm^{-1} . Raman spectra were recorded with Renishaw Raman spectrometer using Ar^+ laser at 514 nm . The morphology and size of the particles were determined from Scanning electron microscope (SEM, Hitachi, S-4300) and transmission electron microscopy (TEM, Hitachi H-7500, operated at 200 kV). For TEM observation, nanopowder was ultrasonically dispersed in ethanol and deposited on a copper-grid supported amorphous holey carbon coil. Optical properties of the synthesized product were monitored using Hitachi, U 3900 H UV–Vis spectrophotometer in the wavelength range 200 – 600 nm . All electrochemical properties were carried out with a CHI-660 instrument.

2.3 Synthesis of GO

GO was synthesized by the oxidation of natural graphite powder using improved Hummer method with a slight modification [27]. Typically, 3.0 g of graphite powder was added to a 4:1 mixture of concentrated $\text{H}_2\text{SO}_4/\text{o-H}_3\text{PO}_4$ (160:40 mL) under constant magnetic stirring. 4.5 g of KMnO_4 was added gradually and the reaction mixture was allowed to stir for 72 h at room temperature to get thick pasty product. Then 200 mL ice cold DI water was slowly poured to the mixture followed by a slow addition of 5 mL H_2O_2 (30%) which led to colour change from dark brown to yellow. The change in colour indicated the formation of GO, which was later confirmed by recording the absorbance spectrum of the solution [28]. The mixture was filtered and washed several times with 1:10 HCl aqueous solution (250 mL) to eliminate the metal ions and acid residue and finally GO dispersion was centrifuged at 3000 rpm for 40 min to remove unexfoliated graphite. The product was allowed to dry at 50°C for 12 h .

2.4 Synthesis of GO/Ag nanocomposites

EG was first heated at 1050°C in air for 15 s . The size was enlarged up to nearly 200 times of its original amount in this procedure. In the present typical procedure for the composite synthesis, first the 50 mg of GO powder was dispersed in 30 mL of EG by sonication for 30 min and kept under the constant stirring for a further 1 h to form GO sheet. Next, 50 , 200 and 350 mg of AgNO_3 was dissolved in 15 mL of EG with 5 mL of DI water. This mixture was then added to GO sheet while stirring and kept at 50°C for 2 h . 40 mL of 0.1 mol/L NaBH_4 solution was slowly added and the mixture was heated at 110°C for 2 h . After complete reduction, the reaction mixture was filtered and the product was washed three times with DI water and then dried in an oven

at 80 °C. These composites were labelled as GO/Ag-1, GO/Ag-2, GO/Ag-3 according to amount of AgNO₃ respectively. The schematic representation of fabrication process of GO/Ag nanocomposites is outlined in Fig. 1.

2.5 Preparation of Go/Ag modified electrode

All the electrochemical experiments were carried out in a three-electrode electrochemical cell system at room temperature. Prior to modification, a glassy carbon disk electrode (GCE) was thoroughly cleaned and polished with alumina (Al₂O₃) slurry (0.005 μm) to obtain mirror like surface. Next, rinsed with DI water, and sonicated in ethanol and doubly distilled water for 15 min. Then the cleaned GCE was dried under nitrogen stream. Platinum (Pt) wire was used as the counter electrode and Ag/AgCl as reference electrode. The GO/Ag-GCE was fabricated by drop-casting, 5 μL of an aqueous GO/Ag solution was allowed to dry at room temperature for an hour. This modified GO/Ag-GCE was denoted as working electrode. For comparison, the GO/GCE was also prepared using the GO dispersion and same procedure as above discussed. 0.1 M phosphate buffer solution (PBS, pH 7.2) was used as a supporting electrolyte for electrochemical experiments.

2.6 Photocatalytic activity of GO/Ag nanocomposites

The visible light catalytic activity of prepared nanocomposites was investigated by reduction of 4-nitrophenol to 4-aminophenol in the presence of NaBH₄. A quartz cuvette with path distance 1 cm and a volume of 2.5 mL was used as a reaction container to analysis the catalytic activity. For the study, an appropriate amount of GO/Ag nanocomposite was added to the aqueous solution containing 0.05 mM of 4-nitrophenol and NaBH₄ (0.25 mg/100 mL) at room temperature to start the reaction. The reduction process was monitored by absorbance measurements with UV–Vis spectrophotometer.

2.7 Mechanism of synthesis of GO/Ag nanocomposites

Among applied approaches for preparing graphene-based composites, those based on utilization of GO are arguably the most versatile and easily scalable methods. GO is a strongly oxygenated, highly hydrophilic layered material that can be readily exfoliated in water to yield stable dispersions consisting mostly of mono-layer GO sheets. These stable flexible GO sheets are usually used as the initial material for the preparation of graphene-based composites [29]. EG is a widely used as a reducing agent. It can not only worked as a chelating agent but also serve as a reducing agent to convert metal ions into metal or alloy nanoparticles [30]. However, since EG is only a mild reducing agent, it requires a long reaction time to reach completion. In this study, we overcome the shortcoming of EG by the addition of a more active reducing agent, NaBH₄. Some amount of DI water was added during the reduction process to facilitate the exfoliation of GO. In addition, the water may buffer the formation rate of the metal particles, and give some control over particle size [31].

3 Results and discussions

3.1 Structural analysis

3.1.1 XRD analysis

The XRD pattern of GO and Go/Ag nanocomposite with different concentration of Ag (Go/Ag-1, GO/Ag-2 and GO/Ag-3) are shown in Fig. 2. As shown in Fig. 2a, GO exhibits a characteristic sharp peak at 2θ value 10.4° corresponding to (002) inter plane due to the presence of oxygen carrying groups on the GO surface [25]. This peak was not shown in GO/Ag nanocomposite due to exfoliation of GO sheet as a result of the Ag nanoparticles surface loading. In the XRD pattern of the GO/Ag nanocomposites Fig. 2b–d, attributes the sharp and well-defined peaks at 2θ values 38.2°, 44.4°, 64.5° and 77.4°, corresponding to the (111),

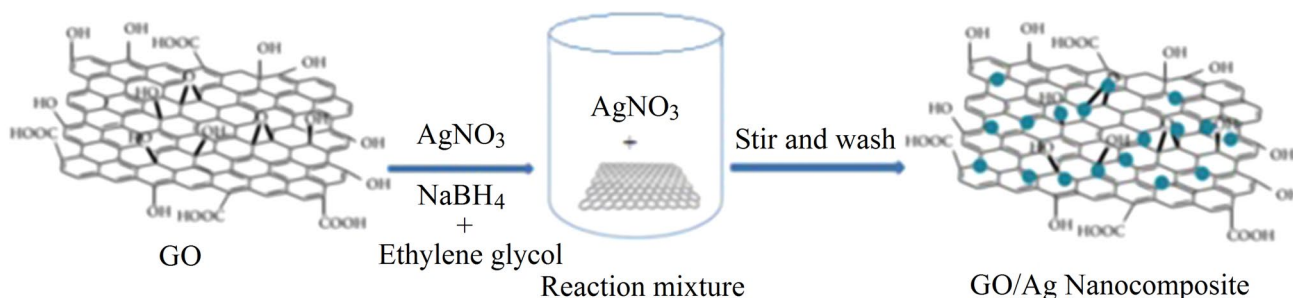


Fig. 1 Schematic representation of fabrication process of GO/Ag nanocomposites

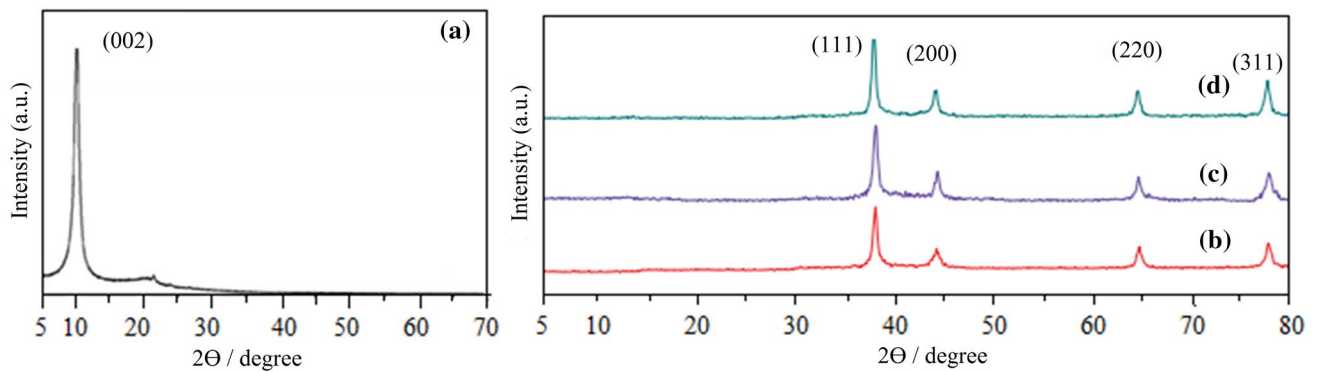


Fig. 2 XRD pattern of GO and GO/Ag nanocomposites **a** GO, **b** GO/Ag-1, **c** GO/Ag-2 and **d** GO/Ag-3

(200), (220), and (311) diffraction planes of the fcc crystal structure for metallic silver (JCPDS File No. 04-0783). The corresponding d-spacing values of the Ag nanoparticles are $d_{111} = 2.37 \text{ \AA}$, $d_{200} = 2.04 \text{ \AA}$, $d_{220} = 1.45 \text{ \AA}$ and $d_{311} = 1.24 \text{ \AA}$ respectively. It is also observed that the d-spacing values of the Ag nanoparticles using different dosage of the AgNO_3 remain almost constant for each crystallographic plane [32]. The intense peak corresponding to $2\theta = 38.2^\circ$ indicates that the obtained Ag nanoparticles are dominantly ruled by (111) plane.

In XRD pattern of GO/Ag nanocomposites, there is no diffraction peak of GO, because the regular stack of GO was destroyed by the intercalation of Ag nanoparticles in nanocomposites [33]. It can be seen from Fig. 2b–d that when the amount of AgNO_3 increased, the intensities of XRD peaks of all samples are gradually close to those of diffraction peaks of crystalline Ag and the full width at half maxima (FWHM) of diffraction peaks become narrow and sharpened, which confirms that the nanoparticles are composed of highly crystalline Ag in Go/Ag nanocomposites

[34]. The average crystallite size of the nanocomposites is calculated from the broadening of the diffraction peak using Debye–Scherrer’s Equation [35].

$$D = 0.9\lambda / \beta \cos \theta \tag{1}$$

where β is the full at width half maximum (radius), λ is the wavelength of Cu K_α (1.5444 \AA) of radiations, θ is Bragg’s angle and D is the crystallite size of the sample. The calculated results from Scherrer formula indicate that the average crystallite sizes of Ag nanoparticles in GO/Ag-1, GO/Ag-2 and GO/Ag-3 are 15.6, 16.4, and 17.9 nm, respectively. It is observed that the size of Ag nanoparticles on surface of GO sheet gradually increased with increasing of the amount of AgNO_3 added.

3.1.2 FTIR analysis

FTIR analysis were carried out in order to identify the presence of various functional groups responsible for the reduction of GO and Ag^+ . Figure 3a shows the FTIR spectra of

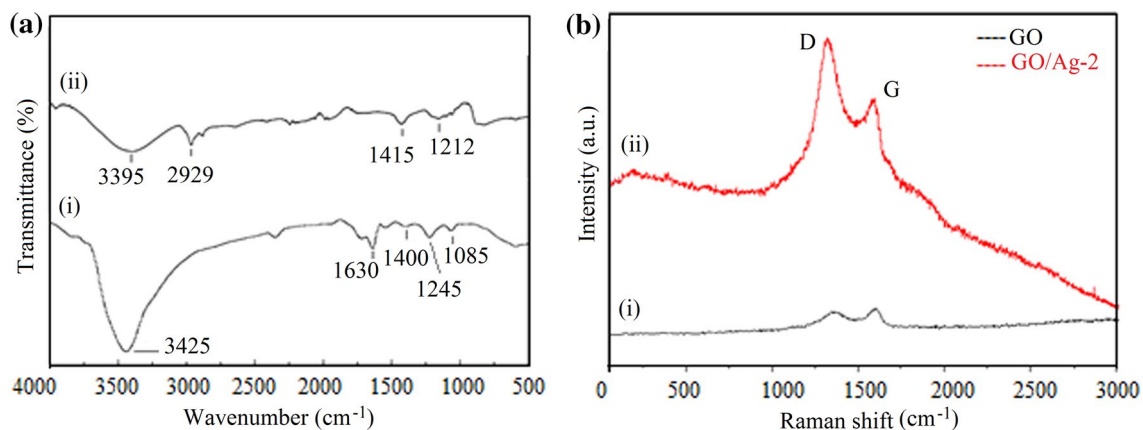


Fig. 3 **a** FTIR spectra of (i) GO and (ii) Go/Ag nanocomposites (GO/Ag-2) and **b** Raman spectra of (i) GO and (ii) Go/Ag nanocomposites (GO/Ag-2)

GO and GO/Ag nanocomposites (GO/Ag-2) in the frequency range of 4000–500 cm^{-1} . It can be seen from (Fig. 3a(i)), the peaks at 3425, 1725, 1630, 1400, 1245 and 1085 cm^{-1} of GO are assigned to the –OH stretching vibrations, C=O stretching of COOH groups, skeletal vibrations of unoxidized graphite domains, O–H deformations of the C–OH groups, epoxy symmetrical ring deformation vibrations and C–O stretching vibrations, respectively [26]. The FTIR spectrum of GO/Ag-2 (Fig. 3a(ii)) shows a broad peak at 3395 cm^{-1} corresponds to O–H stretching vibration of absorbed water molecules, 2929 cm^{-1} corresponds to asymmetric stretching of C–H bonds. Furthermore, the IR peaks at 1415 and 1212 cm^{-1} are attributed for –OH bending of carboxylates and C–OH. The FTIR results revealed that the GO have been successfully exfoliated and reduced to GO sheets. The strong interaction may exist between Ag nanoparticles and the remaining surface hydroxyl groups [36].

3.1.3 Raman spectroscopy analysis

Raman spectroscopy is a most powerful non-destructive micro-analytical technique with single molecule capabilities to characterize carbonaceous materials, especially for distinguishes ordered and disordered carbon structures. Figure 3b shows the Raman spectra of GO and GO/Ag nanocomposites (GO/Ag-2). It was recorded with 514 nm Ar^+ laser excitation. As seen in (Fig. 3b(i)), GO show two peaks at 1349 and 1601 cm^{-1} , which corresponds to the D and G bands, respectively. The D band is assigned to the breathing mode of A_{1g} symmetry involving phonons near the K-zone boundary. The G band is assigned to the E_{2g} mode of sp^2 -bonded carbon atoms [17]. In comparison to the GO, the Raman spectra of GO/Ag-2 (Fig. 3b(ii)) indicates that D and G bands shifted to lower wave numbers at 1347 and 1595 cm^{-1} , respectively. This is due to the reduction of GO during the reaction procedure. In addition, the Raman spectrum of GO/Ag-2 shows a slightly greater I(D)/I(G) intensity ratio (0.946) than that of GO (0.864) [37]. The embedment of Ag nanoparticles on GO sheets may reduce the average size of in-plane sp^2 domains as they encompass a larger degree of surface area of nanometer size when compared to the molecular-sized oxygenous groups of GO. Moreover, the intensity peaks of D and G bands were enhanced in the case of GO/Ag-2 due to the surface enhanced Raman scattering effect from the local electromagnetic fields of Ag nanoparticles that accompanies plasmon resonance [18].

3.2 Morphological studies

The SEM images of GO and Go/Ag nanocomposites with different Ag doping dosage were shown in Fig. 4. It can be observed from Fig. 4a that GO sheet is a closely packed with lamellar structure, mostly plain having drapes between

the sheets. This is due to the cross-linking effect of Π – Π bonds that are easily to make the graphene stack in layered structure [10]. The morphology of GO/Ag nanocomposites (Fig. 4b–d) revealed that the Ag nanoparticles are deposited on GO surface as spacers to keep the neighbouring sheets separate, and a curled, disorganised and corrugated morphology is observed. The size and shape of the Ag nanoparticles are also influenced by the amount of AgNO_3 . In low dosage of AgNO_3 (Fig. 4b), it is difficult to find that Ag nanoparticles are deposited on the GO sheets. After the dosages of AgNO_3 increases to 200 mg (Fig. 4c), the Ag nanoparticles are well separated from each other and distributed randomly on the GO sheets. When AgNO_3 dosages increases to 350 mg (Fig. 4d), the size of Ag nanoparticles increased significantly and nanoparticles tends to agglomerate. Here, the oxygen containing groups on GO sheets provide chemical active centres for Ag attachments and also prevent them from agglomerating. It can be further confirmed by the typical TEM image of as prepared GO/Ag-2. As shown in Fig. 5, well-dispersed, spherical Ag nanoparticles are densely assembled to the surface of GO sheets homogeneously, and the wide size distribution of Ag nanoparticles ranges from 5 to 20 nm. It exhibits its mono- or multi-layer planar sheet-like morphology [38]. Besides, a few of elongated spherical particles are observed in the product which could be resulted from the aggregation of the two or more Ag nanoparticles [39]. The results are also supported by the XRD results.

3.3 Optical characterization

In general, GO contains many functional groups and the formation of GO and GO/Ag nanocomposites can be confirmed by UV–Vis absorption spectroscopy. As shown in Fig. 6a, GO exhibits strong bands centered at 228 nm and the shoulder around 300 nm, which may be ascribed to the $\pi \rightarrow \pi^*$ transition of aromatic C=C bonds and $n \rightarrow \pi^*$ transition of aromatic C=O bonds in GO [40]. The absorption spectra of GO/Ag nanocomposites (GO/Ag-2) revealed that the absorption peak of GO at 228 nm gradually red-shifted to 245 nm, and the shoulder disappeared, which indicates that the extensive conjugated sp^2 -carbon network is restored. Furthermore, it is also noteworthy that a new peak at 412 nm occurred, which can be assigned to the surface plasmon resonance (SPR) absorption band of Ag nanoparticles, suggested the formation of Ag nanoparticles. The single SPR band of the Ag nanoparticles assembled on GO sheet indicated that Ag atoms were grown as smaller sized nanoparticles with almost uniform shape rather than bigger sized or branched nanostructures. GO sheet served as a good host materials for the accommodation of Ag nanoparticles.

In this study, the effect of concentration of GO/Ag nanocomposites (GO/Ag-2) prepared at different concentration

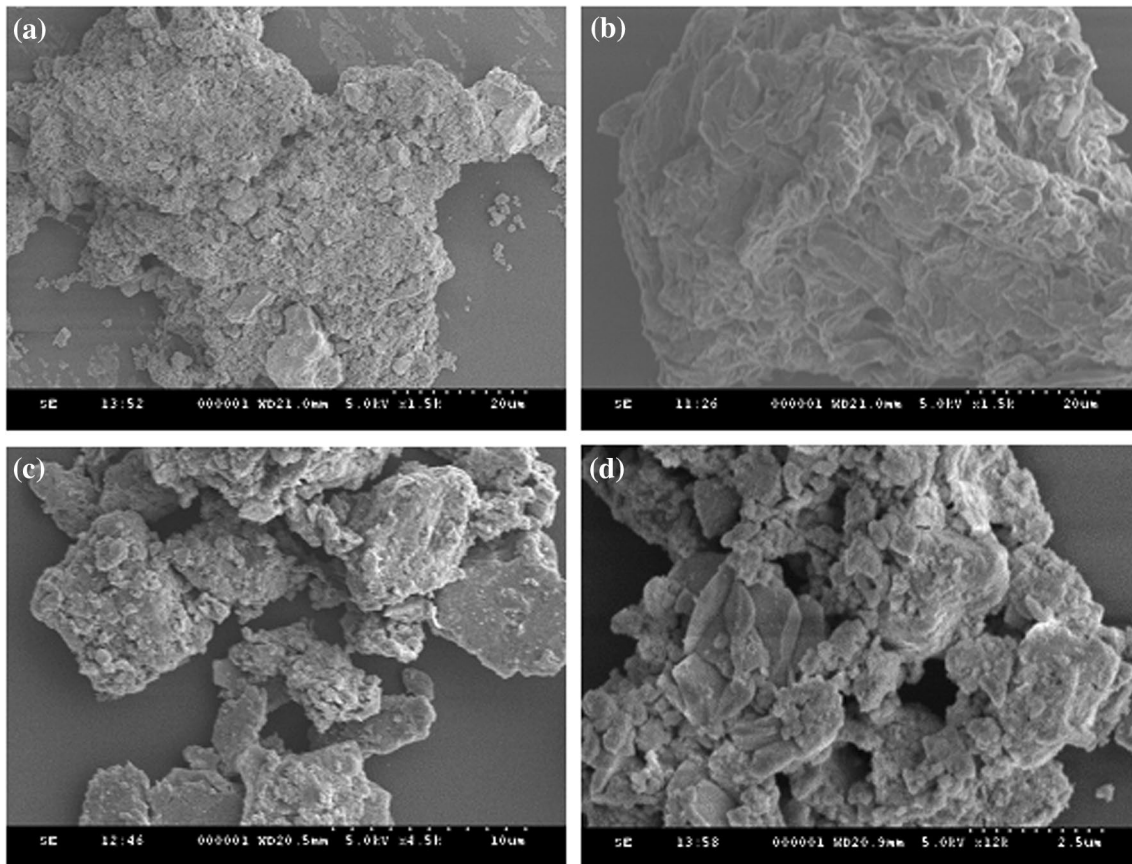


Fig. 4 SEM image of GO and GO/Ag nanocomposites **a** GO, **b** GO/Ag-1, **c** GO/Ag-2 and **d** GO/Ag-3

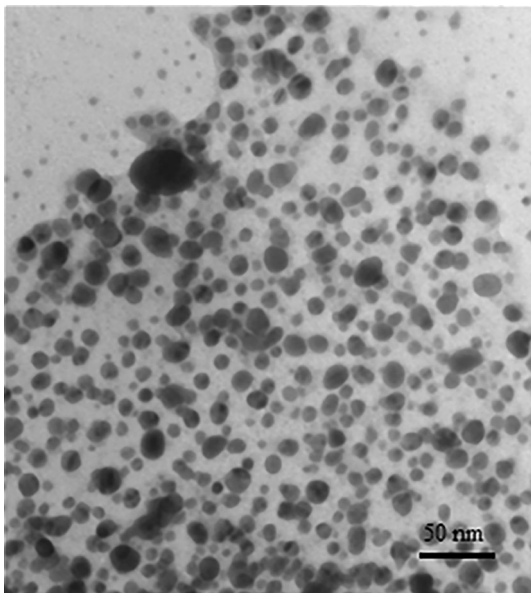


Fig. 5 TEM image of GO/Ag nanocomposites (GO/Ag-2)

(0.1–1.0 mL) was studied (Fig. 6b). At low GO/Ag nanocomposites concentrations (0.1, 0.2 mL), a weak absorption maximum of surface plasmon peak was observed at 412 nm, showing that Ag nanoparticles on GO sheets were produced at a relatively low concentration. With increasing the concentrations, the intensity of the maximum plasmon peak increased, exhibits that higher concentrations of Ag nanoparticles on GO sheets were formed. It is well known that UV–Vis absorption peak can give information on the degree of dispersion of nanoparticles. The narrower the absorption peak, the better the degree of dispersion of nanoparticles [41]. The UV–vis spectra (Fig. 6a, b) are well consist with this statement.

3.4 Electrochemical behaviour of GO/Ag-GCE sensor towards 4-nitrophenol detection

Cyclic voltammetry (CV) was used to determine the electrochemical behaviour of GO/Ag-GCE sensor towards detection of the 4-nitrophenol. Figure 7a shows CVs of GO/Ag-GCE, GO/GCE and GCE in the absence of 4-nitrophenol between the potentials of -0.8 and $+0.8$ V in 0.1 M phosphate-buffered solution (PBS; pH 7.2) at a scan rate of

Fig. 6 UV–Vis spectrum of (a, i) GO, (a, ii) GO/Ag-2, b GO/Ag-2 with different concentrations

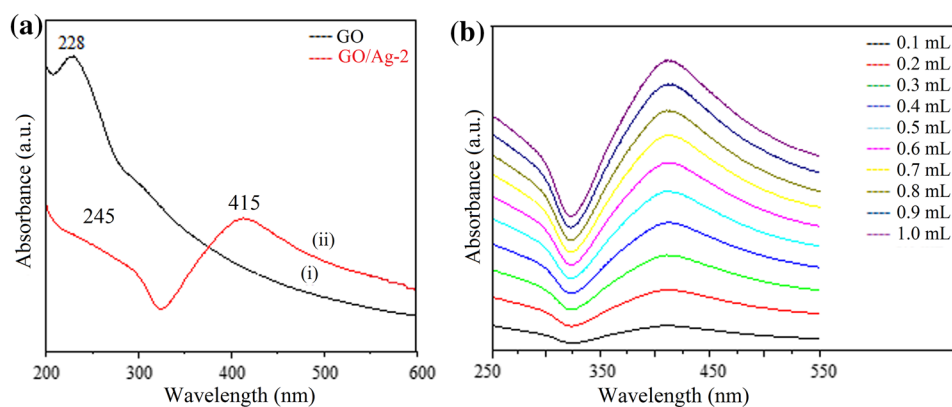
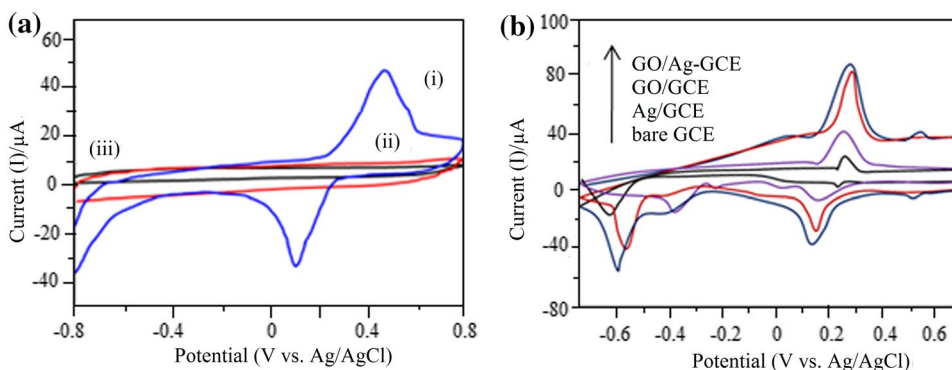


Fig. 7 a CV of (i) GO/Ag nanocomposites (GO/Ag-GCE), (ii) GO/GCE, (iii) GCE in the absence of 4-nitrophenol. b CV of GCE, Ag/GCE, GO/GCE and GO/Ag-GCE containing 1 mM 4-nitrophenol in 0.1 M PBS (pH 7.2) at a scan rate of 50 mV s^{-1}



50 mV s^{-1} which confirms the presence of Ag at the modified electrode surface. There was no redox peak obtained at GCE and GO/GCE without 4-nitrophenol, indicating the GO film is non-electroactive in the selected potential region. The current of GO/GCE was slightly higher than that of GCE, which may be attributed to large specific area of GO [42]. However, a well defined pair of redox peaks was observed for GO/Ag-GCE without 4-nitrophenol, corresponding to Ag/Ag⁺ redox couple. The peak at 0.48 V can be ascribed to the oxidation of Ag (0) → Ag⁺, whereas the reduction of Ag⁺ → Ag (0) exhibits a peak at 0.09 V [43]. This also indicated that Ag nanoparticles have been successfully immobilized onto the GO surface. The proposed GO/Ag-GCE sensor was used for the electrocatalysis and sensing of 4-nitrophenol. When 1 mM 4-nitrophenol was added into the 0.1 M PBS (pH 7.2), at the bare GCE, the redox peaks ascribed to 4-nitrophenol at around 0.32 V were weak, while their intensities progressively increased on GO/Ag-GCE, GO/GCE and Ag/GCE, as shown in Fig. 7b. The results indicated that both Ag nanoparticles and GO had an electrocatalytic activity towards 4-nitrophenol, and GO even owned higher electrocatalytic than Ag nanoparticles. Hence, the synergistic effect of Ag nanoparticles and GO catalyses the electrochemical reaction of 4-nitrophenol [44]. It can be attributed to good catalytic ability and large surface area of GO/Ag-GCE which facilitates the accumulation of the

4-nitrophenol at the surface of electrode and accelerates the electron transfer. Which showed a good sensing nature of GO/Ag-GCE for 4-nitrophenol.

The mechanism of electrochemical oxidation of 4-nitrophenol was presented using CV, in which the potential was cycled from -0.6 to $+0.8$ V, at scan rate of 50 mV s^{-1} . The CV was recorded with GO/Ag-GCE sensor in after presence of 4-nitrophenol (Fig. 8a). It can be seen that the main redox (R₁/O₁) peaks of 4-nitrophenol appeared at 0.18 and 0.24 V respectively. Besides this, 4-nitrophenol shows two pairs of weak redox peaks (O₂/R₂ and O₃/R₃) and two reduction peaks at -0.4 and -0.6 V, both marked by R. The two peaks resulting from the irreversible reduction of the nitro group to produce corresponding hydroxylamine species. The three pairs of redox peaks (O₁/R₁, O₂/R₂ and O₃/R₃) are due to the reversible two-electron oxidation–reduction reaction of 4-aminophenol [28]. The possible electrochemical reactions of 4-nitrophenol on the electrode are described in Fig. 8b (Equations 1–4).

3.5 Photo-catalytic activity

The photocatalytic activities of the GO/Ag nanocomposites (GO/Ag-2) were analyzed by measuring the UV–Vis spectrum through production of 4-aminophenol via 4-nitrophenol reduction under visible light at various times in the presence

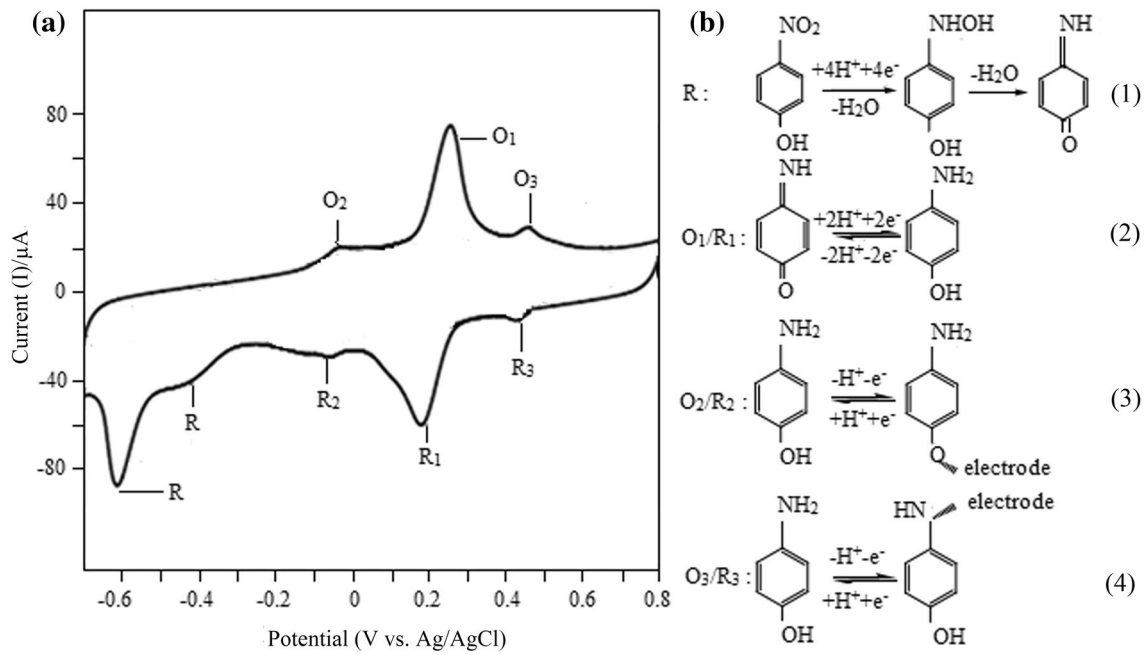
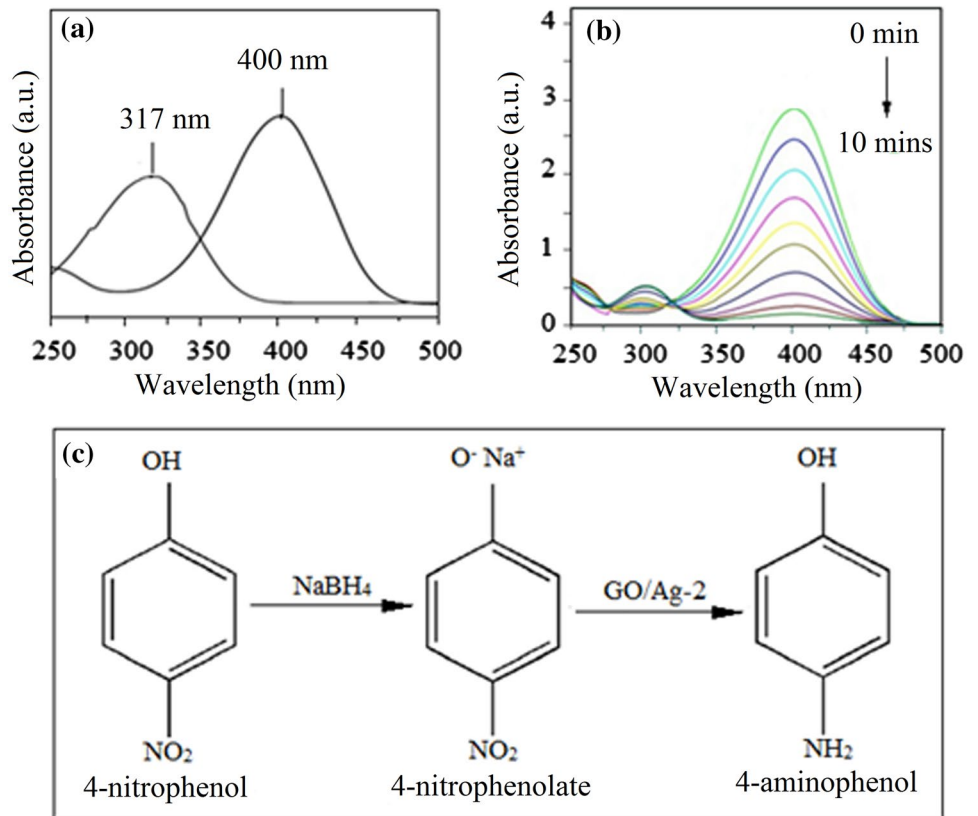


Fig. 8 a CV of the GO/Ag-GCE in the presence of 1 mM 4-nitrophenol in 0.1 M PBS (pH 7.2) at a scan rate of 50 mV s⁻¹. b Proposed 4-nitrophenol electron transfer mechanism

Fig. 9 a UV–Vis spectrum of 4-nitrophenol in the presence and absence of NaBH₄, b time dependent UV–Vis spectra for the reduction of 4-nitrophenol, and c mechanism of photo-catalytic reduction of 4-nitrophenol to 4-aminophenol using GO/Ag₂ nanocomposite (GO/Ag-2)



of NaBH_4 at room temperature. Figure 9a shows, in the absence of GO/Ag nanocomposites, a peak at 317 nm corresponds to 4-nitrophenol, is the electronic transition $n-\pi^*$, owing to the lone pair of electrons (oxygen and nitrogen atoms) in the 4-nitrophenol structure. This peak shifted to a higher wavelength at 400 nm after the addition of NaBH_4 , attributes to 4-aminophenol, which is the reduction product of 4-nitrophenol [45]. The solution colour transformed from light yellow to yellow-green after adding the NaBH_4 . The reaction took place in presence of NaBH_4 leading to the formation of 4-nitrophenolate ion by conversion of 4-nitrophenol to 4-aminophenol (Fig. 9c). Figure 9b shows the addition of GO/Ag nanocomposites led to a rapid reduction of 4-nitrophenol. The intensity of absorption at 400 nm decreased for 4-nitrophenol, while a new peak simultaneously appeared at 300 nm corresponding to 4-aminophenol in the time-domain UV–Vis spectra [46].

When GO/Ag nanocomposites are exposed to visible light, the electron–hole pairs will be produced in Ag nanoparticles due to its SPR phenomenon. Then the electrons will transfer into GO sheet by the interface between Ag nanoparticles and GO. The two dimensional planar conjugation structure of GO facilitate charge transfer along the GO sheets to electron acceptors like oxygen molecules, and thus an effective charge separation is achieved. O_2^- radicals will be produced by the reduction of oxygen molecules adsorbed onto GO surface by the photo generated electrons which are very powerful oxidizing agents and can degrade 4-nitrophenol effectively under visible-light [10]. The mechanism of photocatalytic degradation of 4-nitrophenol to 4-aminophenol by GO/Ag nanocomposites with NaBH_4 is as shown in Fig. 9c. It can be concluded from previous reports that the GO/Ag nanocomposites possess enhanced catalytic activity compared with the Ag nanoparticles. The reduction rate of the composites is much higher than that of pure Ag nanoparticles and comparable to other substrate-supported Ag nanocatalysts [46, 47]. The high activity of GO/Ag nanocomposites may be attributed to the GO support. Since GO with large surface area is dispersed well in aqueous solution. This leads to highly efficient contact between 4-nitrophenol and Ag nanoparticles on GO. Moreover, the stability of Ag nanoparticles in the reaction was enhanced because of the presence of GO [48].

4 Conclusions

In brief, a facile simple one pot reduction method was proposed for the preparation of GO/Ag nanocomposites using EG and NaBH_4 . GO was acted as a substrate and stabilizer to prepare synthesized nanocomposites. The GO/Ag nanocomposites were successfully characterized by XRD, FTIR, Raman spectroscopy, SEM, TEM and UV–Vis absorption

spectroscopy. Fabricated GO/Ag–GCE sensor showed a good sensing and catalytic ability towards 4-nitrophenol. The GO/Ag nanocomposites showed excellent catalytic activity and stability for the reduction of 4-nitrophenol to 4-aminophenol with NaBH_4 . It was revealed that the GO played important role in the high activity and stability of the hybrids. The as-prepared GO/Ag nanocomposites hold enormous ability to degrade the 4-nitrophenol from the environment.

Acknowledgements The authors are highly thankful to Director, CSIR-Central Scientific Instruments Organisation (CSIR-CSIO), Chandigarh (INDIA) for permitting us to carry out this research work.

References

1. X. Feng, Y. Zhang, J. Zhou, Y. Li, S. Chen, L. Zhang, Y. Ma, L. Wang, X. Yan, Three dimensional nitrogen-doped graphene as an ultrasensitive electrochemical sensor for the detection of dopamine. *Nanoscale* **7**, 2427–2432 (2015)
2. C. Lee, X. Wei, J.W. Kysar, J. Hone, Measurement of the elastic properties and intrinsic strength of monolayer graphene. *Science* **321**, 385–388 (2008)
3. A.A. Balandin, S. Ghosh, W. Bao, I. Calizo, D. Teweldebrhan, F. Miao, C.N. Lau, Superior thermal conductivity of single-layer graphene. *Nano Lett.* **8**, 902–907 (2008)
4. X. Feng, Y. Zhang, J. Song, N. Chen, J. Zhou, Z. Huang, Y. Ma, L. Zhang, L. Wang, MnO₂/Graphene nanocomposites for nonenzymatic electrochemical detection of hydrogen peroxide. *Electroanalysis* **27**, 353–359 (2015)
5. K. Haubner, J. Murawski, P. Olk, L.M. Eng, C. Ziegler, B. Adolph, E. Jaehne, The route to functional graphene oxide. *Chem. Phys. Chem.* **11**, 2131–2139 (2010)
6. R. Pasricha, S. Gupta, A.G. Joshi, N. Bahadur, K.N. Sood, S. Singh, Directed nanoparticles reduction on graphene. *Mater. Today* **15**, 118–125 (2012)
7. H.P. Cong, J.J. He, Y. Lu, S.H. Yu, Water-soluble magnetic-functionalized reduced graphene oxide sheets: in situ synthesis and magnetic resonance imaging applications. *Small* **6**, 169–173 (2010)
8. M. Heidarizad, S.S. Sengor, Synthesis of graphene oxide/magnesium oxide nanocomposites with high-rate adsorption of methylene blue. *J. Mol. Liq.* **224**, 607–617 (2016)
9. N. Kumar, A.K. Srivastava, H.S. Patel, B.K. Gupta, G.D. Varma, Facile synthesis of ZnO–reduced graphene oxide nanocomposites for NO₂ gas sensing applications. *Eur. J. Inorg. Chem.* **11**, 1912–1923 (2015)
10. H.L. Jun, W.Y. Xin, T.J. Guo, W. Yao, L.J. Xian, J.J. Qing, W. We, Preparation of graphene/silver nanohybrid composite with good surface-enhanced Raman scattering characteristics. *Int. J. Electrochem. Sci.* **11**, 398–405 (2016)
11. R. Fu, M. Zhu, Synthesis and characterization of structure of Fe₃O₄@graphene oxide nanocomposites. *Adv. Comp. Lett.* **25**, 143–146 (2016)
12. J. Xie, X. Yang, X. Xu, C. Yang, Microwave synthesis of reduced graphene oxide-supported platinum nanocomposite with high electrocatalytic activity for methanol oxidation. *Int. J. Electrochem. Sci.* **12**, 466–474 (2017)
13. Y.Z. Zhou, J. Yang, X. Cheng, N. Zhao, H. Suna, D. Li, Transparent and conductive reduced graphene oxide/silver nanoparticles multilayer film obtained by electrical self-assembly process with graphene oxide sheets and silver colloid. *RSC Adv.* **3**, 3391–3398 (2013)

14. Y.L. Shao, Y. Shao, H. Wang, Q. Zhang, Y. Li, High-performance flexible asymmetric supercapacitors based on 3D porous graphene/MnO₂ nanorod and graphene/Ag hybrid thin-film electrodes. *J. Mater. Chem. C* **1**, 1245–1251 (2013)
15. K.C. Hsu, D.H. Chen, Green synthesis and synergistic catalytic effect of Ag/reduced graphene oxide nanocomposite. *Nanoscale Res. Lett.* **9**, 484 (2014)
16. Q. Li, X. Qin, Y. Luo, W. Lu, G. Chang, A.M. Asiri, A.O. Al-Youbi, X. Sun, One-pot synthesis of Ag nanoparticles/reduced graphene oxide nanocomposites and their application for nonenzymatic H₂O₂ detection. *Electrochim. Acta* **83**, 283–287 (2012)
17. M. Zainy, N.M. Huang, S.V. Kumar, H.N. Lim, C.H. Chia, I. Harrison, Simple and scalable preparation of reduced graphene oxide-silver nanocomposites via rapid thermal treatment. *Mater. Lett.* **89**, 180–183 (2012)
18. A.M. Golsheikh, N.M. Huang, H.N. Lim, R. Zakaria, C.Y. Yin, One-step electrodeposition synthesis of silver nanoparticles decorated graphene on indium-tin-oxide for enzymeless hydrogen peroxide detection. *Carbon* **62**, 405–412 (2013)
19. L. Liu, J.C. Liu, Y.J. Wang, X.L. Yan, D.D. Sun, Facile synthesis of monodispersed silver nanoparticles on graphene oxide sheets with enhanced antibacterial activity. *New J. Chem.* **35**, 1418–1423 (2011)
20. L. Fu, Y. Zheng, Z. Wang, A. Wang, B. Dengand, F. Peng, Facile synthesis of Ag-AgCl/ZnO hybrid with high efficiency photocatalytic property under visible light. *Dig. J. Nanomater. Biostruct.* **10**, 117–124 (2015)
21. A. Niaziand, A. Yazdanipour, Spectrophotometric simultaneous determination of nitrophenol isomers by orthogonal signal correction and partial least squares. *J. Hazard. Mater.* **146**, 421–427 (2007)
22. C. Nistor, A. Oubiña, M.P. Marco, D. Barceló, J. Emnéus, Competitive flow immunoassay with fluorescence detection for determination of 4-nitrophenol. *Anal. Chim. Acta* **426**, 185–195 (2001)
23. E. Dorta, M. González, M.G. Lobo, C. Sánchez-Moreno, B.D. Ancos, Screening of phenolic compounds in by-product extracts from mangoes (*Mangifera indica* L.) by HPLC-ESI-QTOF-MS and multivariate analysis for use as a food ingredient. *Food Res. Int.* **57**, 51–60 (2014)
24. L. Fu, Y.H. Zheng, Z.X. Fu, Ascorbic acid amperometric sensor using a graphene-wrapped hierarchical TiO₂ nanocomposite. *Chem. Pap.* **69**, 655–661 (2015)
25. E. Salih, M. Mekawy, R.Y.A. Hassan, I.M. El-Sherbiny, Synthesis, characterization and electrochemical-sensor applications of zinc oxide/graphene oxide nanocomposite. *J. Nanostruct. Chem.* **6**, 137–144 (2016)
26. G. Yang, One-pot preparation of reduced graphene oxide/silver nanocomposite and its application in the electrochemical determination of 4-nitrophenol. *Int. J. Electrochem. Sci.* **10**, 9632–9640 (2015)
27. D.C. Marcano, D.V. Kosynkin, J.M. Berlin, A. Sinitskii, Z. Sun, A. Slesarev, B.A. Lawrence, W. Lu, M. James. Tour, Improved synthesis of graphene oxide. *ACS Nano* **4**, 4806–4814 (2010)
28. S. Singh, N. Kumar, M. Kumar, A. Agarwal, B. Mizaiakoff, Electrochemical sensing and remediation of 4-nitrophenol using bio-synthesized copper oxide nanoparticles. *Chem. Eng. J.* **313**, 283–292 (2017)
29. M.J. McAllister, J.L. Li, D.H. Adamson, H.C. Schniepp, A.A. Abdala, J. Liu, M.H. Alonso, D.L. Milius, R. Car, R.K. Prud'homme, I.A. Aksay, Single sheet functionalized graphene by oxidation and thermal expansion of graphite. *Chem. Mater.* **19**, 4396–4404 (2007)
30. K.T. Jeng, C.C. Chien, N.Y. Hsu, S.C. Yen, S.D. Chiou, S.H. Lin, W.M. Huang, Performance of direct methanol fuel cell using carbon nanotube-supported Pt–Ru anode catalyst with controlled composition. *J. Power Sources* **160**, 97–104 (2006)
31. W.Z. Li, C.H. Liang, W.J. Zhou, J.S. Qiu, H.Q. Li, G.Q. Sun, Q. Xin, Homogeneous and controllable Pt particles deposited on multi-wall carbon nanotubes as cathode catalyst for direct methanol fuel cells. *Carbon* **42**, 436–439 (2004)
32. W. Yuan, Y. Gu, L. Li, Green synthesis of graphene/Ag nanocomposites. *Appl. Surf. Sci.* **261**, 753–758 (2012)
33. M.R. Das, R.K. Sarma, R. Saikia, V.S. Kale, M.V. Shelke, P. Sengupta, Synthesis of silver nanoparticles in an aqueous suspension of graphene oxide sheets and its antimicrobial activity. *Colloids Surf. B* **83**, 16–22 (2011)
34. M.G. Naseri, E. Saion, N.K. Zadeh, The amazing effects and role of PVP on the crystallinity, phase composition and morphology of nickel ferrite nanoparticles prepared by thermal treatment method. *Int. Nano Lett.* **3**, 1–8 (2013)
35. M. Kumar, P. Devi, A. Kumar, Structural analysis of PVP capped silver nanoparticles synthesized at room temperature for optical, electrical & gas sensing properties. *J. Mater. Sci.* **28**, 5014–5020 (2017)
36. R.V. Hull, L. Li, Y.C. Xing, C.C. Chusuei, Pt nanoparticles binding on functionalized multiwalled carbon nanotubes. *Chem. Mater.* **18**, 1780–1788 (2006)
37. Y. Zhou, J. Yang, X. Cheng, N. Zhao, L. Sun, H. Sun, D. Li, Electrostatic self assembly of graphene-silver multilayer films and their transmittance and electronic conductivity. *Carbon* **50**, 4343–4350 (2012)
38. J.C. Meyer, A.K. Geim, M. Katsnelson, K. Novoselov, T. Booth, S. Roth, The structure of suspended graphene sheets. *Nature* **446**, 60–63 (2007)
39. L. Huang, H. Yang, Y. Zhang, W. Xiao, Study on synthesis and antibacterial properties of Ag NPs/GO nanocomposites. *J. Nanomater.* 1–9 (2016) Article ID 5685967
40. S.J. Wang, Y.W. Zhang, H.L. Ma, Q.L. Zhang, M.L. Zhai, Ionic-liquid-assisted facile synthesis of silver nanoparticle-reduced graphene oxide hybrids by gamma irradiation. *Carbon* **55**, 245–252 (2013)
41. K.D. Kim, D.N. Han, H.T. Kim, Optimization of experimental conditions based on the Taguchi robust design for the formation of nano-sized silver particles by chemical reduction method. *Chem. Eng. J.* **104**, 55–61 (2005)
42. R.A. Dar, N.G. Khare, D.P. Cole, S.P. Karna, A.K. Srivastava, Green synthesis of a silver nanoparticles-graphene oxide composite and its application for As (III) detection. *RSC Adv.* **4**, 14432–14440 (2014)
43. J. Li, D. Kuang, F. Zhang, Z. Xu, M. Liu, D. Wang, Green synthesis of silver nanoparticles–graphene oxide nanocomposite and its application in electrochemical sensing of tryptophan. *Biosens. Bioelectron.* **42**, 198–206 (2013)
44. M. Welch, R. Christine, G. Compton, The use of nanoparticles in electroanalysis: a review. *Anal. Bioanal. Chem.* **3**, 601–619 (2006)
45. J. Li, C.Y. Liu, Y. Liu, Au/graphene hydrogel: synthesis, characterization and its use for catalytic reduction of 4-nitrophenol. *J. Mater. Chem.* **22**, 8426–8430 (2012)
46. Y. Li, Y. Cao, J. Xie, D. Jia, H. Qin, Z. Liang, Facile solid-state synthesis of Ag/graphene oxide nanocomposites as highly active and stable catalyst for the reduction of 4-nitrophenol. *Catal. Commun.* **58**, 21–25 (2015)
47. M.F. Merino, L. Guardia, J. Paredes, S.V. Rodil, A.M. Alonso, J. Tascon, Developing green photochemical approaches towards the synthesis of carbon nanofiber- and graphene-supported silver nanoparticles and their use in the catalytic reduction of 4-nitrophenol. *RSC Adv.* **3**, 18323–18331 (2013)
48. Y. Wan, Y. Wang, J. Wu, D. Zhang, Graphene oxide sheet-mediated silver enhancement for application to electrochemical biosensors. *Anal. Chem.* **83**, 648–653 (2010)